NASA CONTRACTOR REPORT NASA CR-159421

EMISSION MEASUREMENTS FOR A LEAN PREMIXED PROPANE/AIR SYSTEM AT PRESSURES UP TO 30 ATMOSPHERES

By Gerald Roffe and K. S. Venkataramani

(NASA-CR-159421) EMISSION MEASUREMENTS FOR A LEAN PREMIXED PROPANE/AIR SYSTEM AT PRESSURES UP TO 30 ATMOSPHERES Final Report (General Applied Science Labs., Inc.) 41 p HC A03/MF A01 CSCL 21B G3/25

N79-10165

Unclas 33851

Prepared by

GENERAL APPLIED SCIENCE LABORATORIES, INC.
Westbury, New York 11590

For Lewis Research Center
NAS3-20603

NATIONAL AERONAUTICS AND SPACE ADMINISTRATION, WASHINGTON D.C.
JUNE 1978

41 08

1. Report No.	2. Government Accession No.	3. Recipient's Catalog No.
CR-159421		

4. Title and Subtitle	5. Report Date
Emission Measurements for a Lean Premixed Propane/Air System at Pressures up to 30 Atmospheres	AUGUST 1978
	6. Performing Organization Code

7. Author(s)	8. Performing Organization Report No.
Gerald Roffe & K. S. Venkataramani	GASL TR 250
	10. Work Unit No.

9. Performing Organization Name and Address	11. Contract or Grant No.
General Applied Science Laboratories, Inc. Merrick and Stewart Avenues Westbury, New York 11590	NAS3-20603
	13. Type of Report and Period Covered

12. Sponsoring Agency Name and Address	
Airbreathing Engines Division NASA Lewis Research Center 21000 Brookpark Road, Cleveland, Ohio 44135	CONTRACTOR REPORT 14. Sponsoring Agency Code

15. Supplementary Notes

Final Report, Project Manager, Robert Duerr, Airbreathing Engines Division, NASA Lewis Research Center, Cleveland, Ohio 44135. Supplemental to "Experimental Study of the Effect of Cycle Pressures on Lean Combustion Emissions." NASA CR-3032.

16. Abstract

A series of experiments were conducted in which the emissions of a lean premixed system of propane/air were measured in a flametube apparatus. Tests were conducted at inlet temperatures of 600K and 800K and pressures of 10 atm and 30 atm over a range of equivalence ratios. The data obtained were combined with previous data taken in the same apparatus to correlate NO_x emissions with operating conditions. NO_x emission index was found to be well represented by the expression:

$$\ln\left(\frac{E_{NO_x}}{\tau}\right) = -72.28 + 2.80\sqrt{T} - \frac{T}{38.02}$$

where T is the adiabatic flame temperature (K) and τ is the combustor residence time (msec). The expression is independent of pressure over the range of 5 atm to 30 atm for inlet air temperatures of 727K and higher.

Sampling probe design was found to have a pronounced effect on measured CO levels but did not influence NO_x measurements. The most effective probe tested was one which combined thermal and pressure quenching of the gas sample.

17. Key Words (Suggested by Author(s))		18. Distribution Statement
Premixing	Gas Turbine Combustors	
Combustion	Primary Zones	
Oxides of Nitrogen	Gas Sampling Probes	

19. Security Classif. (of this report)	20. Security Classif. (of this page)
UNCLASSIFIED	UNCLASSIFIED

* For sale by the National Technical Information Service, Springfield, Virginia 22161

NASA-C-168 (Rev. 10-75)

TABLE OF CONTENTS

LIST OF FIGURES

INTRODUCTION

In a recently completed experimental program described in Reference (1), the emissions of a lean premixed prevaporized propane-air combustion system were measured over a matrix of inlet temperature and pressure. The matrix included inlet temperatures of 600, 800 and 1000K and pressures of 5, 10, 20 and 30 atm. Matrix points at which data were obtained are indicated in Table I, below:

TABLE I

T \ P	5 atm	10 atm	20 atm	30 atm
600K	*	*	*	U
800K	*	*	*	*
1000K	*	*	F	F

Matrix points marked with asterisks in Table I indicate conditions at which data were obtained. Those points marked with the letter F indicate conditions at which attempts to operate produced flashback. The letter U at the 30 atm/ 600K operating point indicates that combustion at this condition was unstable. with the flame oscillating between the flameholder and a station near the exhaust throat.

Table I indicates that relatively little data was obtained at the 30 atm operating condition. Since operation at pressures of at least 30 atm is anticipated for future engines, there is considerable interest in obtaining additional data on LPP combustion at this condition. This report describes a brief series of experiments in which the premixing combustion apparatus employed in Reference (1) was modified to produce stable combustion at 30 atm

---

Ref. 1. Roffe, G. and Venkataramani, K. S., "Experimental Study of the Effects of Cycle Pressure on Lean Combustion Emissions," NASA CR 3032, July 1978.

pressure. Emissions data were taken at this pressure for entrance temperatures of 600K and 800K. Emissions measurements were also made at a pressure of 10 atm, again for entrance temperatures of 600 and 800K, these latter tests prompted by a desire to obtain additional data at a condition where considerable data scatter was reported in Reference (1).

APPARATUS

Test Rig - The combustion test rig is illustrated schematically in Figure (1). Heated dry air enters the apparatus through the bellmouth, passing through an instrumentation spool where the entrance temperature and pitot-static pressure profiles are measured by an embedded rake. Fuel enters the device through a heated plenum chamber which surrounds the instrumentation spool and feeds fifty-two individual 1.6 mm diameter injection tubes. The tubes extend 7 cm downstream from their entry point and inject fuel in the streamwise direction to minimize the possibility of local flow separation. The relatively long and thin injection tubes are supported at their midpoints by a fine honeycomb structure 6 mm in streamwise extent representing a flow blockage of 3%. The fuel injector assembly is shown in Figure (2).

The mixer tube is constructed of a heavy outer pressure wall and a thin stainless steel liner. The two elements are separated by an internally vented air gap to minimize heat loss. Four thermocouples are mounted 90^{o} apart 2.5 cm from the downstream end of the mixer and placed so that their tips are flush with the inner surface of the liner. The thermocouples serve as indicators of autoignition in the mixer or flashback through the flameholder.

The flameholder assembly is illustrated in Figure (3). The flameholder is a water-cooled perforated plate, employing 21 holes 0.95 cm in diameter to produce a porosity of 22%. At the 25 m/s reference velocity used in this experiment, the flameholder produces a total pressure drop of 3%. It is provided with two wall surface thermocouples on the downstream surface and one on the upstream surface and an integral hydrogen-air igniter which is used to initiate combustion. Flameholder depth, measured in the streamwise direction, is 1.6 cm.

The combustor assembly also employs a double wall design to protect the heavy outer pressure wall. Here the air gap between the combustor liner and the outer carbon steel wall is kept cool by injecting a small amount of cold air. In addition, an alumina tube is mounted inside the stainless steel liner as illustrated in Figure (4) to provide an uncooled refractory combustor wall, minimizing convective and radiative losses from the gas.

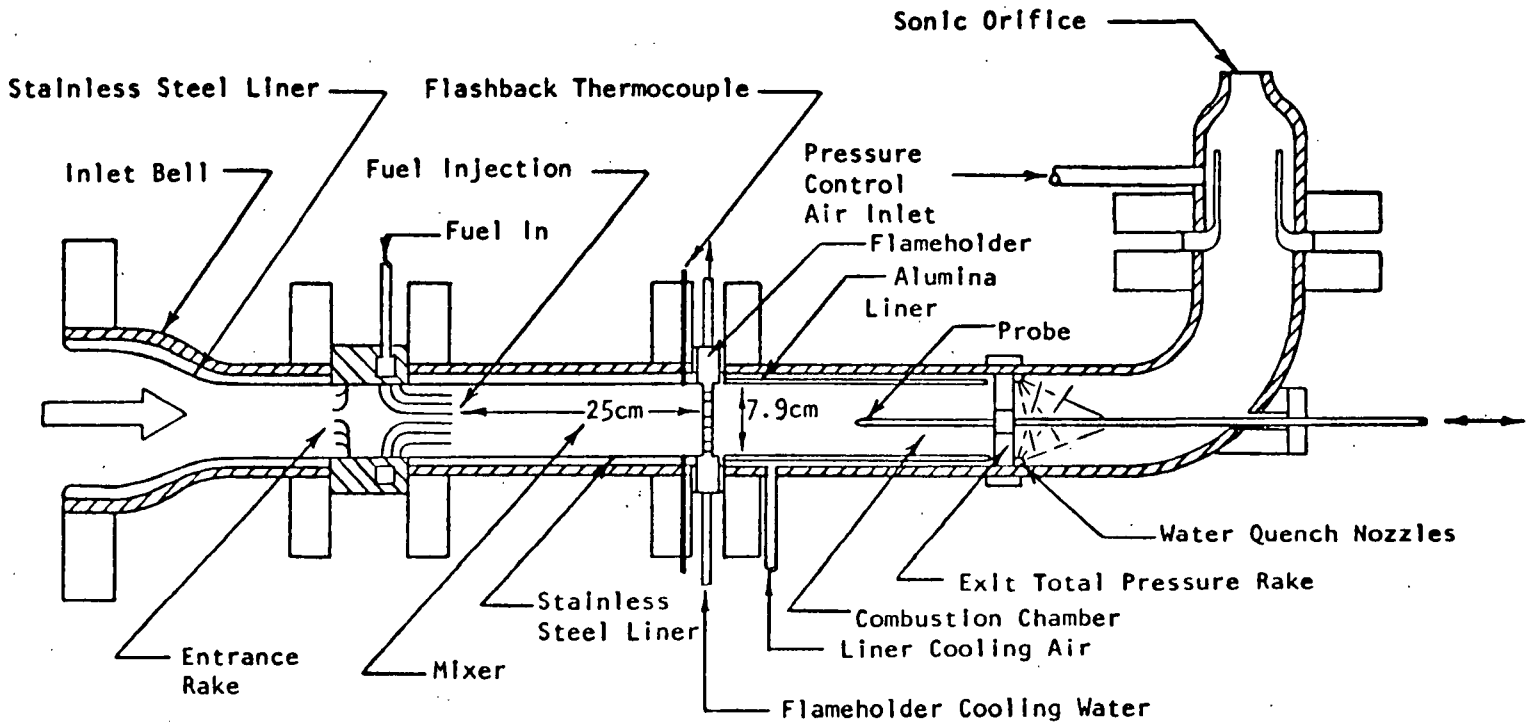

FIGURE 1. COMBUSTION TEST RIG

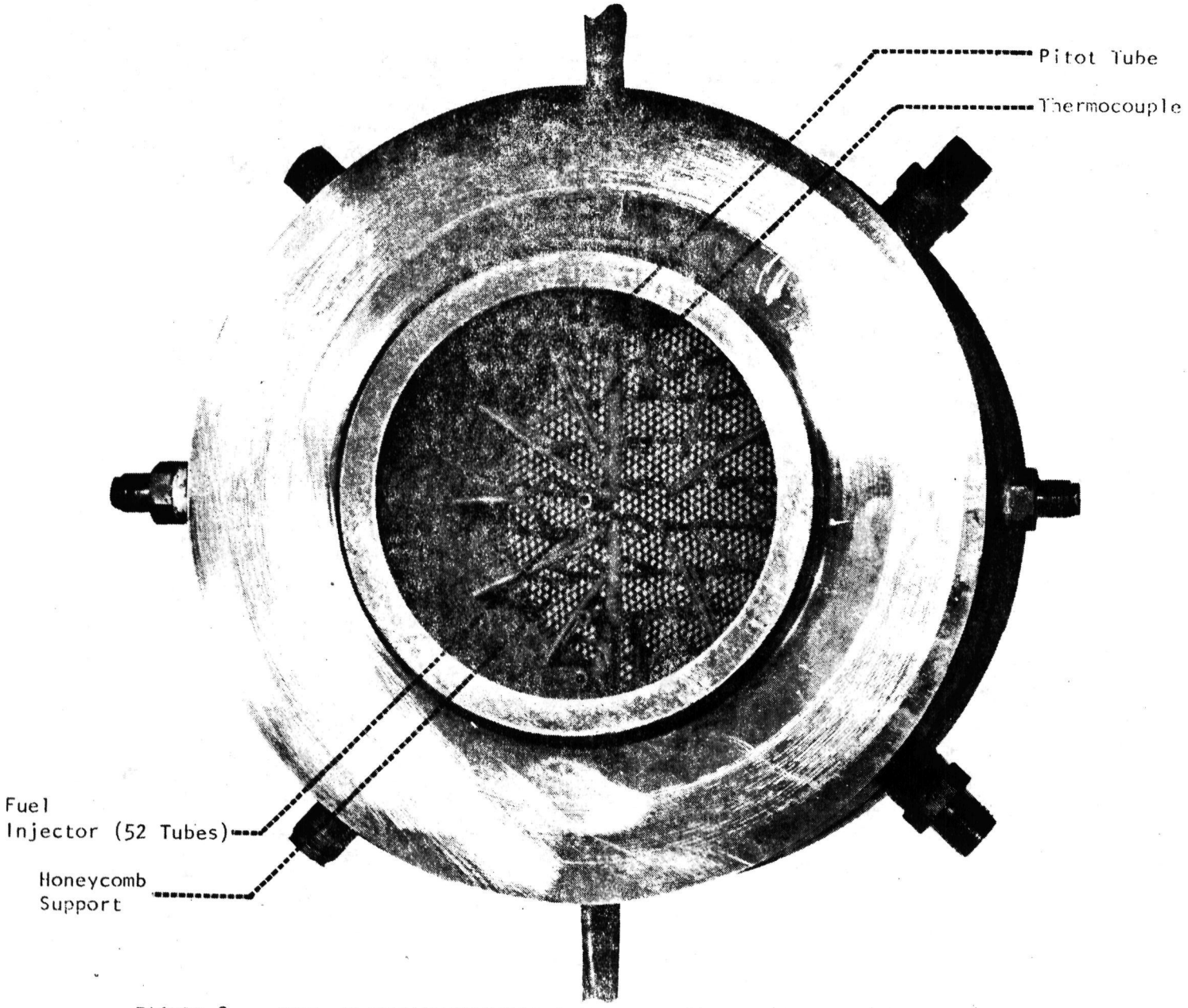

FIGURE 2. FUEL INJECTION/FORWARD INSTRUMENT SPOOL ASSEMBLY (VIEWED FROM UPSTREAM SIDE)

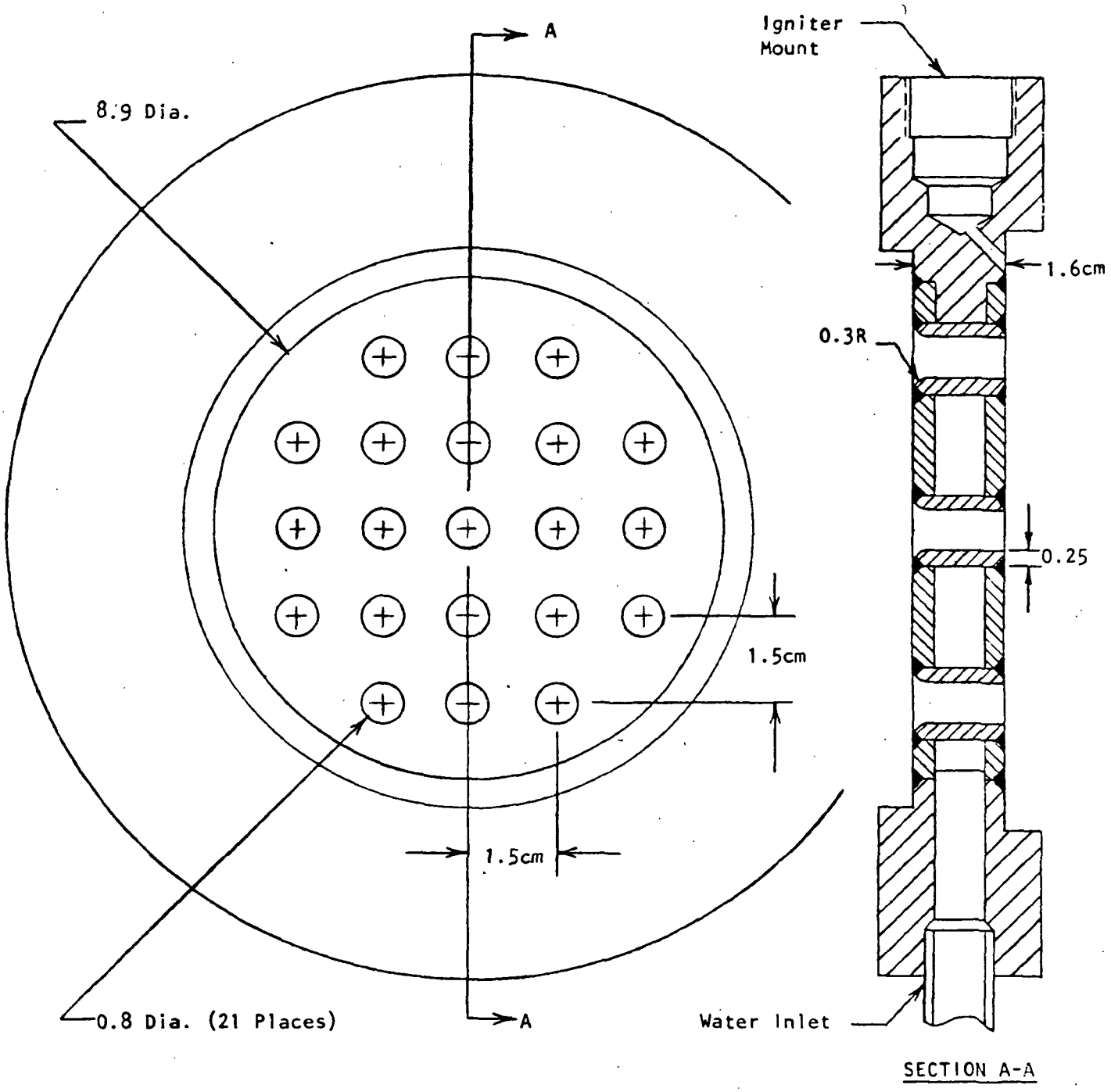

FIGURE 3. WATER-COOLED PERFORATED PLATE FLAMEHOLDER

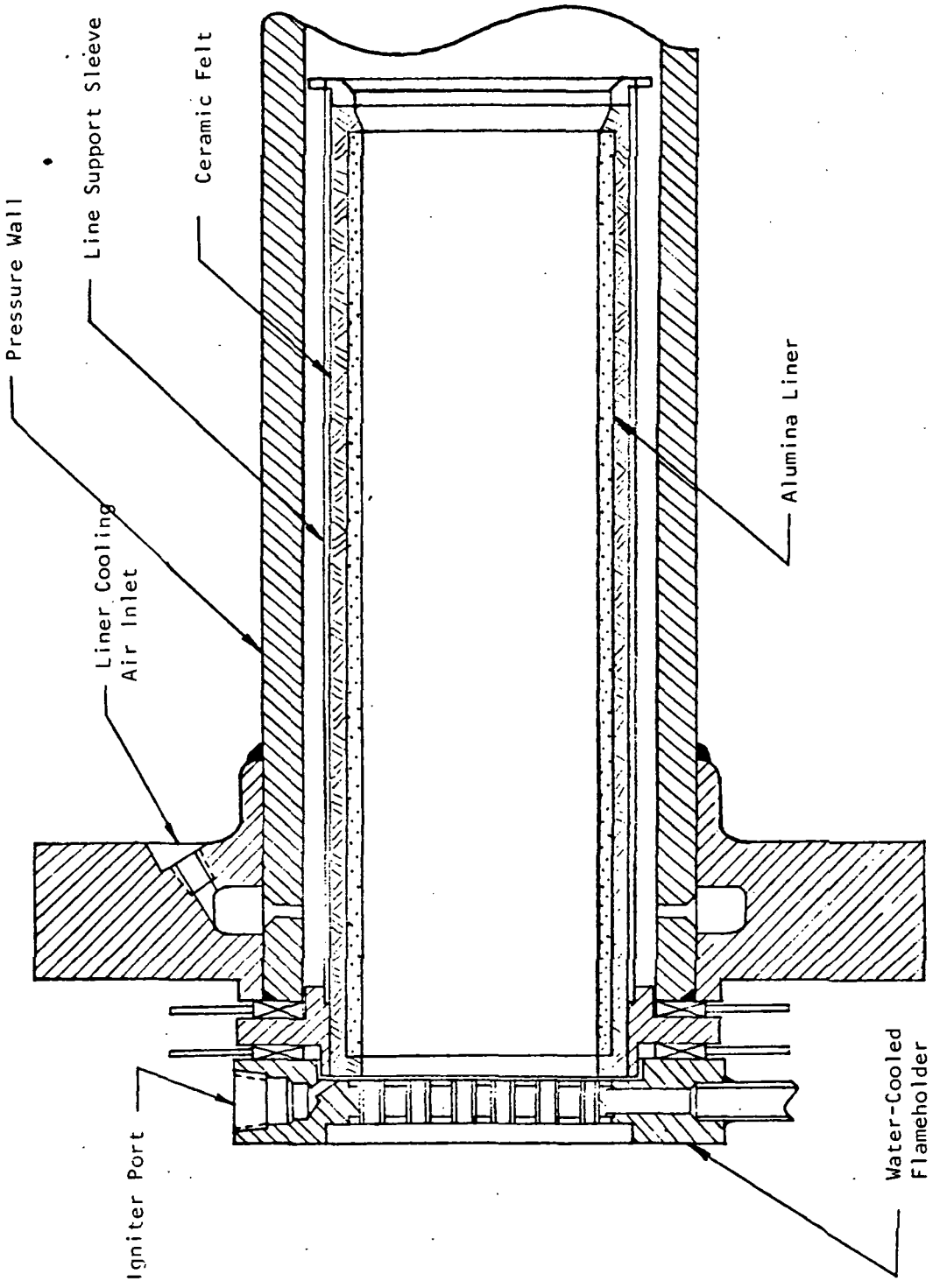

FIGURE 4. DETAILS OF COMBUSTOR CONSTRUCTION

A dome-loaded pressure regulator is used to supply cold air to an annular injection section just upstream of the rig exit orifice. By loading the regulator to the pressure desired for the test, the appropriate amount of cold air is added automatically to produce the correct total pressure in the test rig. This method of pressure control offers the dual advantages of automatic compensation for varying combustor exit temperature and thermal protection for the choked exit orifice.

Fuel System and Fuel Properties - The fuel supply system is illustrated schematically in Figure (5). Liquid propane is stored in a tank and pressurized with nitrogen. The liquid is withdrawn from the lower section of the supply tank, passing through a turbine flowmeter and pressure regulator before entering a cavitating venturi which provides a constant fuel mass flow rate independent of downstream pressure fluctuations. Fuel flow rate is controlled during a test by adjusting the regulated pressure on the upstream side of the cavitating venturi. The propane is heated to a temperature of 395K in a pressurized water bath and passed through a heated line to a metering venturi before being delivered to the injection plenum. An analysis of the commercial grade propane used in these experiments is presented in Table II.

Test Procedure - In operation, the air flow through the rig is established at the desired temperature and at a mass flow rate corresponding to a 25 m/sec reference velocity at the test pressure and temperature. The rig pressure is then brought up to the operating value by injection of an appropriate amount of cold air at the exit orifice. The gas igniter is turned on, fuel flow initiated and slowly increased until ignition is achieved. The rig equivalence ratio is brought to the highest level desired during the particular test sequence, the gas igniter shut off and the rig operated to assure steady conditions. Gas samples are then withdrawn at a combustor location corresponding to a residence time of two milliseconds. The combustor location which corresponds to this residence time is calculated from the 25 m/sec mixer tube reference velocity and the fuel/air ratio, assuming an instantaneous jump in temperature from the entrance value to the adiabatic flame temperature. Once data has been obtained at a given equivalence ratio, fuel flow rate is lowered and

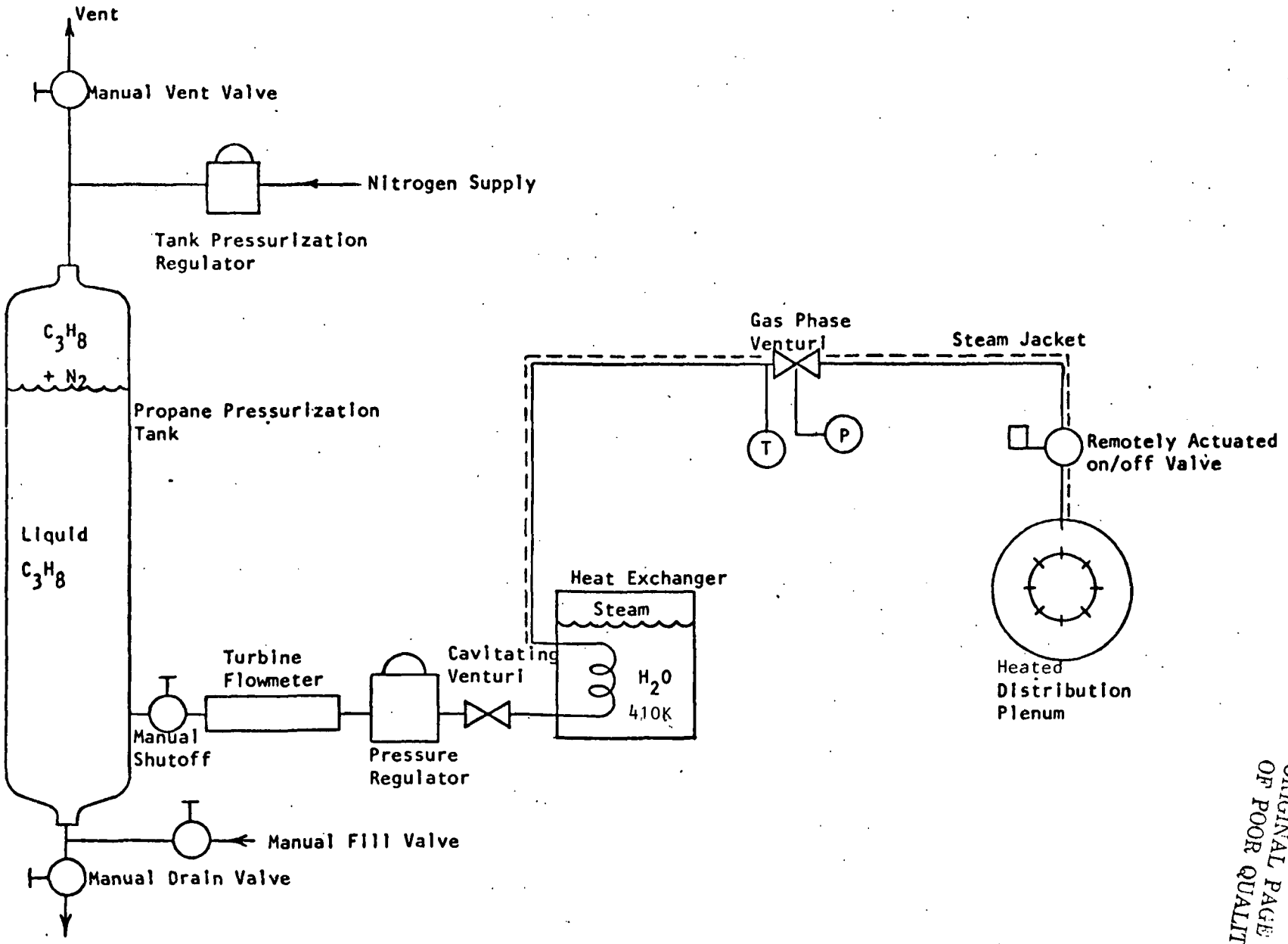

FIGURE 5. PROPANE STORAGE AND DELIVERY SYSTEM SCHEMATIC

TABLE II

ANALYSIS OF COMMERCIAL GRADE PROPANE USED IN TEST PROGRAM

Property	Value
% Propane	90
% Butane	0.084
% Ethylene and Ethane	0.034
% Propylene	9.2
% Volatile Sulfur	0.0073
Specific Gravity (air ≡ 1.0)	1.541
Vapor Pressure, MPa	0.85
Hydrogen/Carbon Atom Ratio	2.597

the sampling probe moved to the new two millisecond position. The process is repeated until the lean stability limit is reached, either extinguishing the flame or producing CO levels beyond the range of the instrumentation.

The apparatus used here is essentially identical to that used for the experiments reported in Reference (1). However, as that rig proved incapable of holding a steady flame at the 30 atm/600K operating condition, a number of modifications were made for the present tests. These consisted of increasing the temperature of the steam bath in the propane vaporization heat exchanger to 410K and installing electric resistance heaters on the fuel distribution plenum to preclude the possibility of liquid-phase fuel reaching the mixer section; modifying the gas-phase venturi in the fuel line to better isolate the upstream and downstream flow volumes; and increasing the mass flow of hydrogen and air to the maximum stable limit in the gas igniter. A heated gas-phase fuel storage reservoir was also inserted between the heat exchanger and the gas-phase venturi. However,, initial tests of the rig demonstrated that while combustion stability was unaffected by this reservoir, fuel system response time was undesirably increased. The reservoir was removed from the fuel system prior to final emissions testing.

Instrumentation - The design of the sampling probe constitutes an extremely important element of the experiment, particularly for the high pressure conditions of interest here. It is necessary for chemical reactions in the gas sample to be slowed to an acceptable level as soon after the sample enters the probe as possible in order to avoid errors associated with residence time. This problem is particularly severe in the case of carbon monoxide whose oxidation reactions are pressure accelerated and further speeded by the high OH concentrations present. The difficulty here is associated with the sample quenching process. As the sample is cooled, the equilibrium concentration of CO decreases. If the sample quenching rate is too slow, CO levels will drop during the cooling process, attempting to remain in equilibrium.

Three sampling probe designs were evaluated during this test series: one based entirely on thermal quenching and two based on a combination of pressure and thermal quenching. The thermal quench probe design is illustrated in

Figure (6). The probe consists of a hollow 1.27 cm diameter sheath terminating in a hemispheric tip through which a 1 mm diameter sampling hole is drilled. The gas sample flows through the tip into a 1.6 mm diameter tube which carries it out of the probe. The 1.6 mm sample tube is jacketed by an intermediate tube through which cooling water enters the probe. The water flows past the probe tip, returning through the annular gap between the intermediate tube and the probe sheath. The cooling water is exhausted outside the combustion apparatus. The flow path of the cooling water is such that its temperature is as low as possible where it contacts the sample delivery tube. In addition, the small delivery tube diameter produces rapid cooling of the gas which it carries.

Figure (7) illustrates the first pressure-quench sampling probe design which employs only a moderate degree of thermal quenching. Here, the gas entering the probe through the 1.6 mm sampling port is expanded into a 6 mm diameter dump tube within which the pressure is maintained at 2 atm. Since the reactions of interest here are all pressure-accelerated, the rapid drop in pressure produces an immediate reduction in reaction rates. Shortly after the expansion station, a portion of the gas is withdrawn through a 1.6 mm sampling tube immersed in the water cooling passage between the probe sheath and the dump tube. In this design, the cooling water moves in only one direction and is exhausted into the combustor through holes in the sheath.

The third design, illustrated in Figure (8), employs a greater degree of thermal quench along with the basic pressure-quench technique. Here, gas from the 1 mm sampling port expands into a 3.2 mm dump tube within which the pressure is maintained at two atmospheres. A portion of this gas is withdrawn through a 1.6 mm quenching tube which extends through a water delivery tube to the probe exit. The sample quenching tube protrudes to the centerline of the dump tube to avoid capturing gas which may have been either recirculated or wall-catalyzed. The water turns at the probe tip and returns to the probe exit as it cools the outer sheath.

The gas sample analysis system and data reduction techniques are described in detail in Reference (1). The entire system conforms to the requirements of SAE ARP 1256.

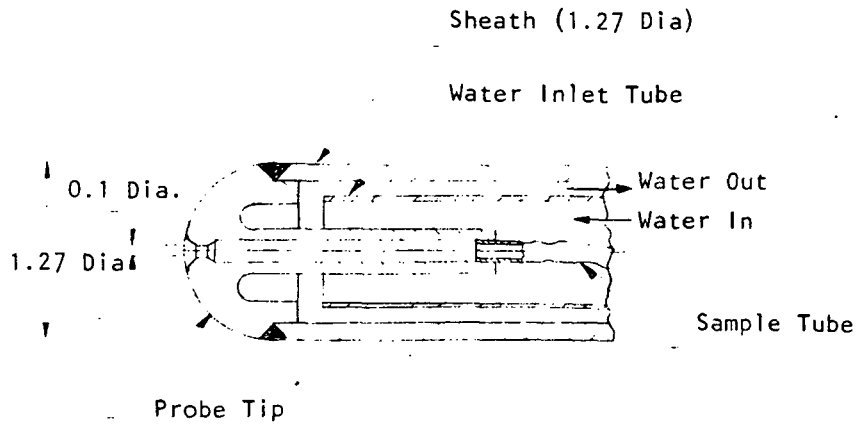

(Dimensions in cm.)

FIGURE 6. THERMAL QUENCH PROBE

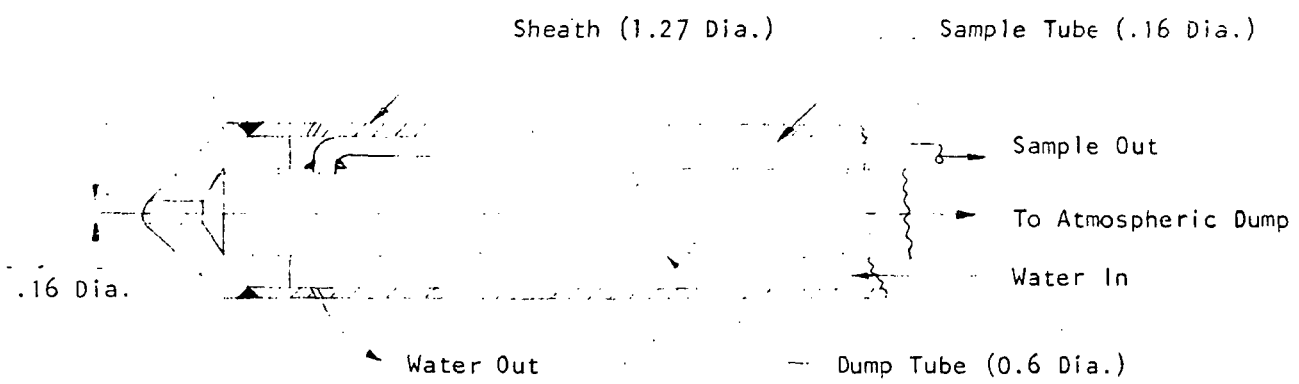

FIGURE 7 PRESSURE REDUCTION SAMPLING PROBE WITH MODERATE THERMAL QUENCH

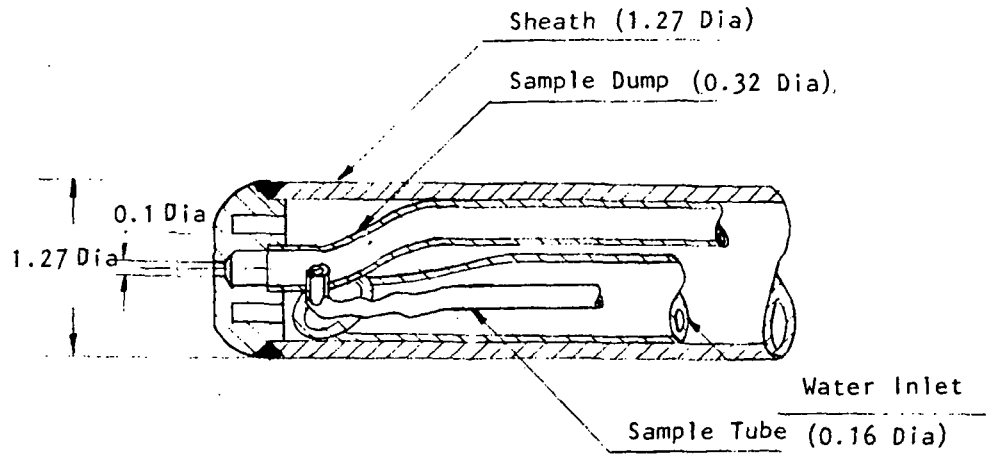

(Dimensions in cm.)

FIGURE 8. PRESSURE/THERMAL-QUENCH PROBE

RESULTS

The three sampling probes were first tested at inlet conditions of 10 atm and 800K using an uncooled perforated plate flameholder to determine the most suitable design for higher pressure testing. Each probe was mounted at a fixed position 30 cm downstream of the flameholder and gas samples withdrawn as equivalence ratio was varied between 0.35 and 0.75. The test sequence was repeated for each of the probes. The results of these tests are presented in Figure (9).

Measured CO level is seen to be a strong function of probe design. The pressure-reduction probe with moderate thermal quench delivers the lowest CO concentration to the analyzers. The thermal-quench probe produces higher CO levels, although its performance is similar to that of the pressure-quench design at the higher equivalence ratios where heating load increases. The pressure/thermal quench probe delivers by far the highest CO levels to the analyzer, particularly at high equivalence ratio.

Measured NO_x level is seen to be independent of probe design, repeating remarkably well for the three test sequences. Unburned hydrocarbon levels, which are below the minimum accuracy level of the hydrocarbon analyzer until just before the lean blowout limit, do not provide a suitable medium of comparison although the data obtained using the three probes does appear consistent.

From these results it would appear that although NO_x and UHC measurements are not strong functions of sampling probe design, CO measurements most definitely are. The large difference between the pressure/thermal and straight thermal quenching design indicates the performance improvement which accrues from providing a rapid pressure reduction. The poor performance of the pressure-quench design employing only moderate thermal quenching indicates that considerable care must be taken to assure that the pressure reduction step is followed by effective sampling cooling. Based on the results of these probe evaluation measurements, the pressure/thermal quench sampling probe was selected for use in the remainder of the test program although even this design delivers CO levels which were somewhat lower than those for chemical equilibrium under conditions of

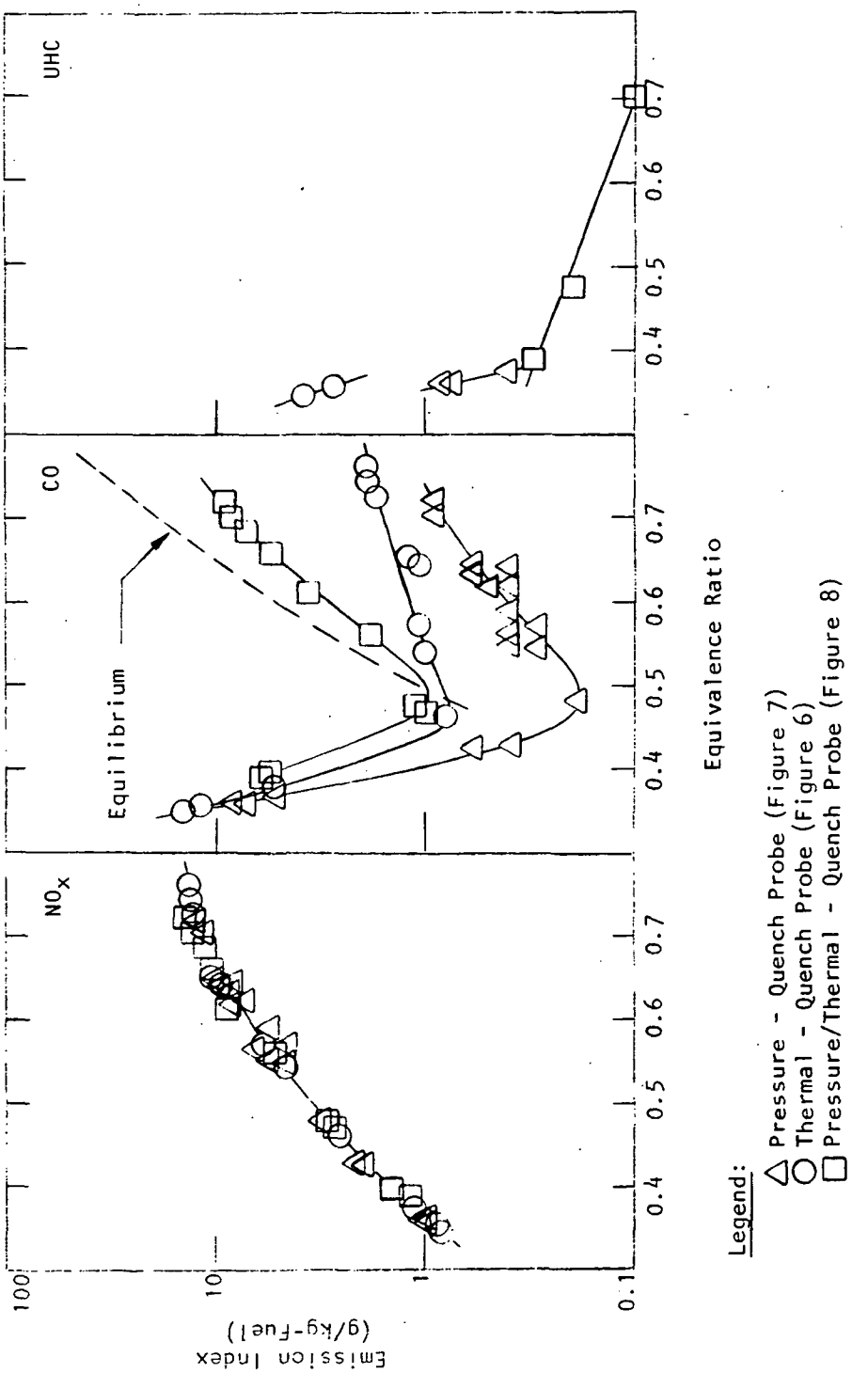

FIGURE 9. COMPARISON OF EMISSIONS MEASUREMENTS USING THERMAL, PRESSURE AND PRESSURE/THERMAL QUENCH PROBE DESIGNS. (T = 800K, p = 10 atm.)

very high adiabatic flame temperature where one normally presumes chemical equilibrium to exist.

The emissions measurements at 30 atm pressure at 600K and 800K entrance temperature are presented in Figures (10) and (11). Measurements at 10 atm pressure and 600K and 800K entrance temperature are presented in Figures (12) and (13). All data is summarized in tabular form in the Appendix.

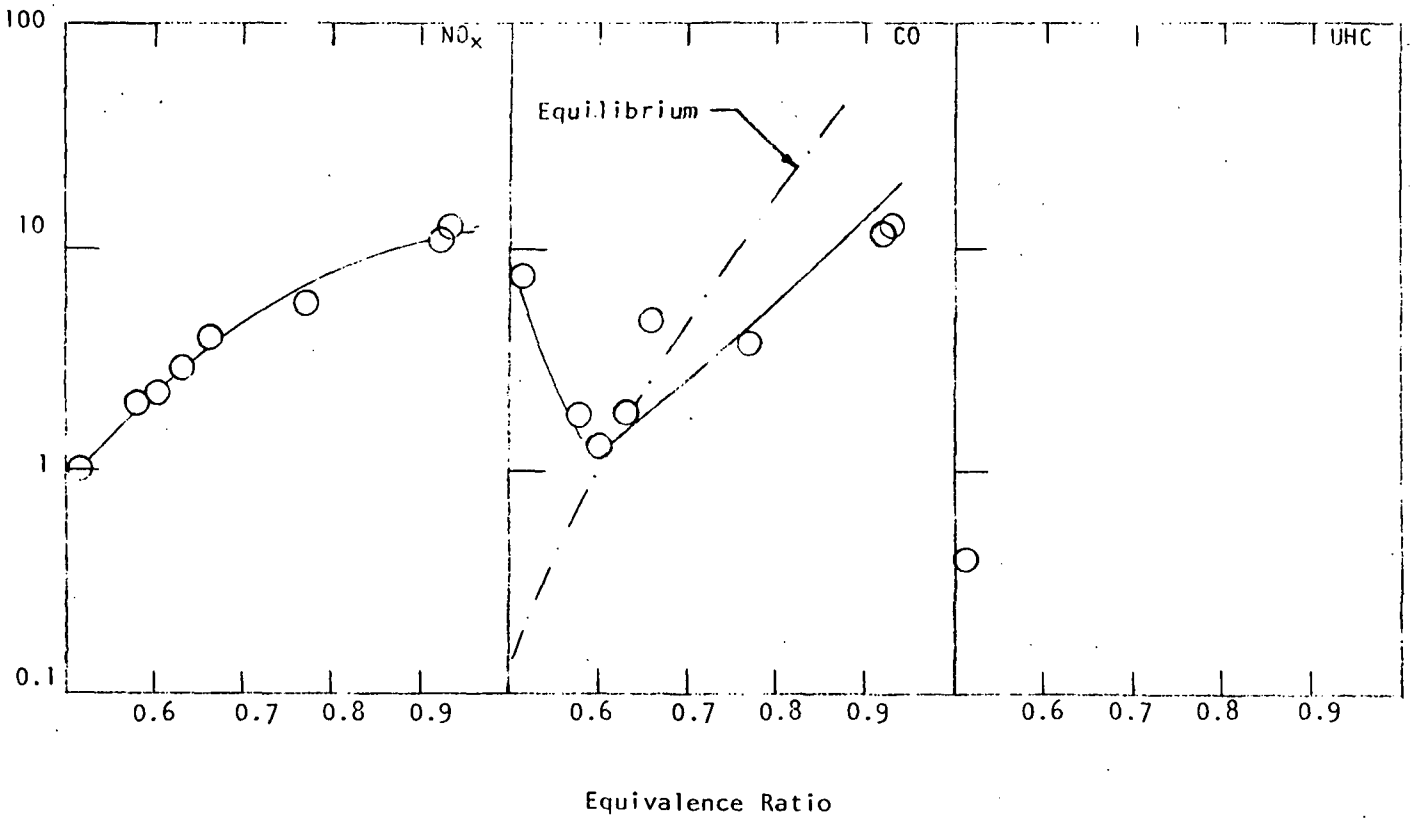

Inlet Temperature = 600K

Inlet Pressure = 30 atm

Residence Time = 2 msec

FIGURE 10. EMISSION MEASUREMENTS

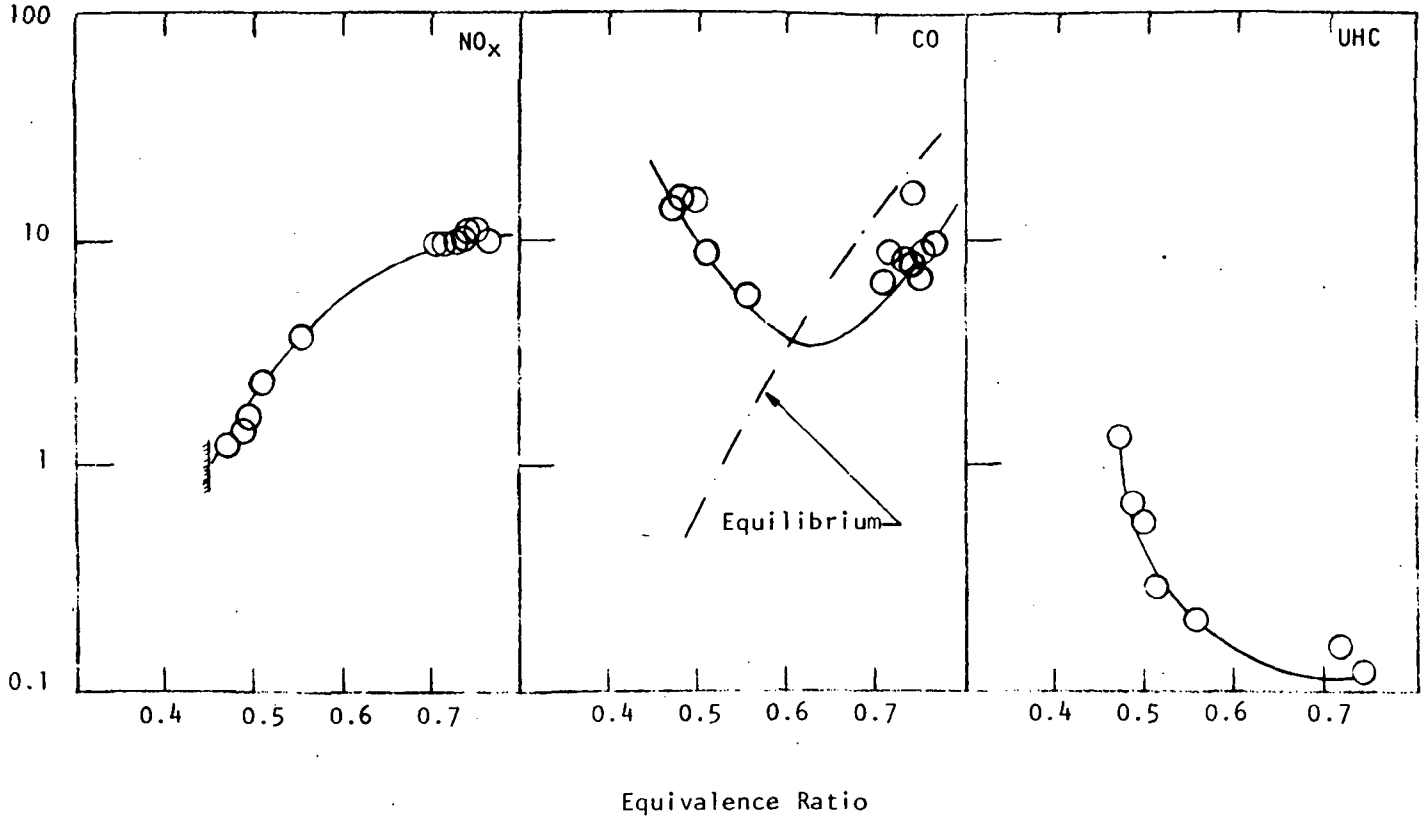

Inlet Temperature = 800K

Inlet Pressure = 30 atm

Residence Time = 2 msec

FIGURE 11. EMISSION MEASUREMENTS

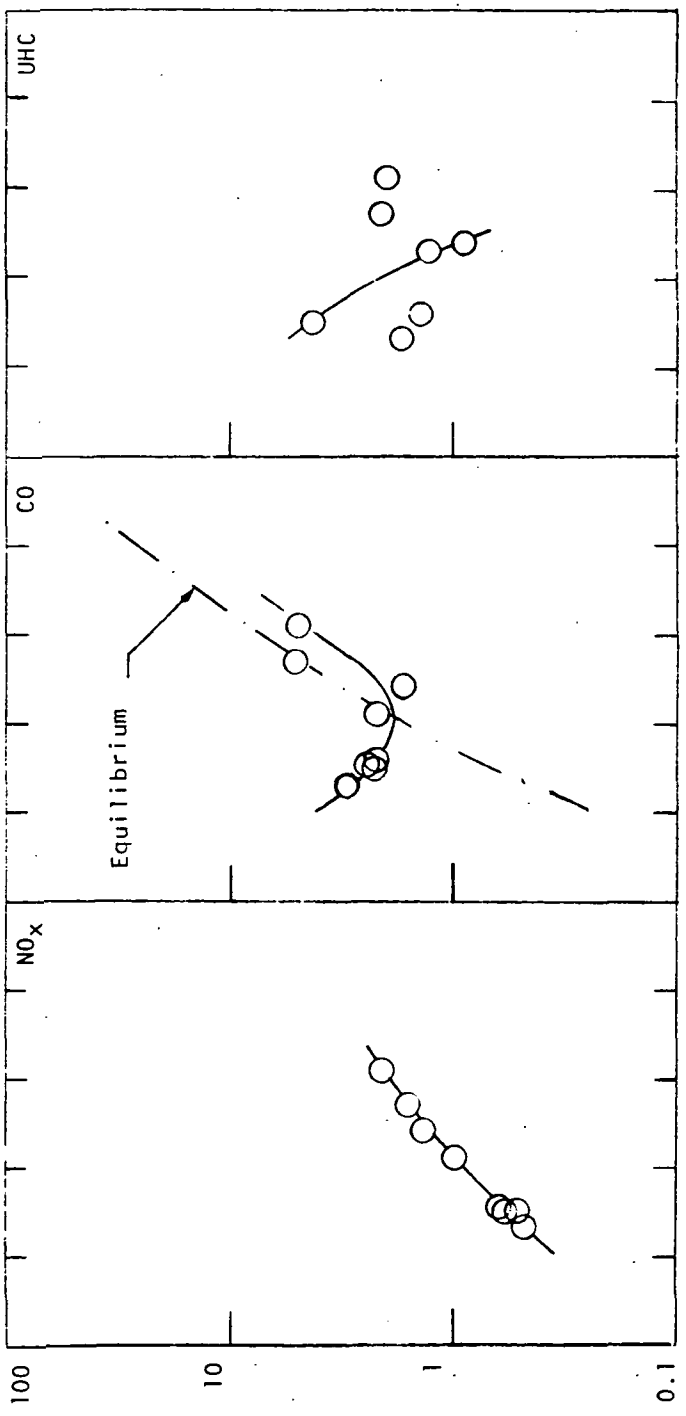

FIGURE 12. EMISSION MEASUREMENTS

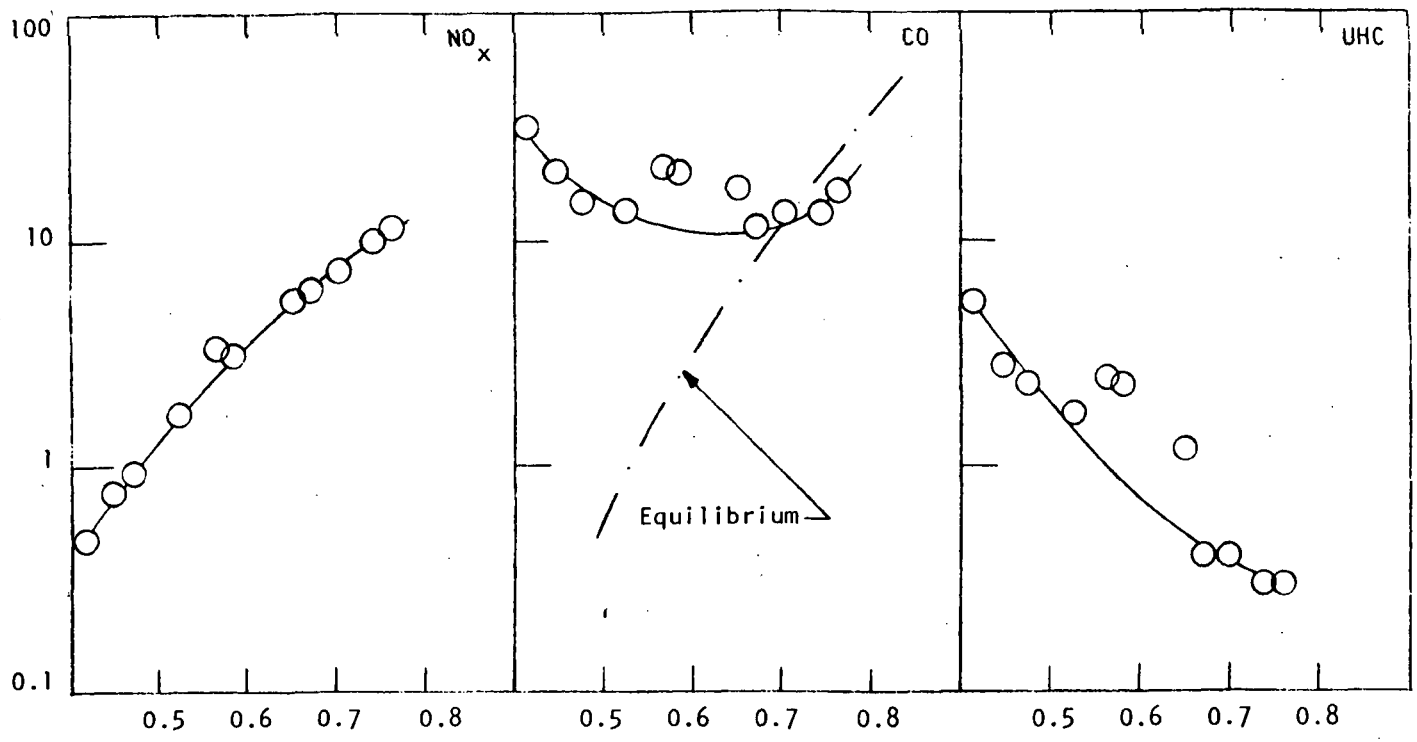

Inlet Temperature = 800K

Inlet Pressure = 10 atm

Residence Time = 2 msec

FIGURE 13. EMISSION MEASUREMENTS

DISCUSSION OF RESULTS

Since NO_x production is basically a post-flame reaction, one would expect it to be a strong function of adiabatic flame temperature. Accordingly, the NO_x emission index measured at 30 atm has been replotted as a function of adiabatic flame temperature with the results shown in Figure (14). Here, the present data for entrance temperature of 600K and 800K are seen to collapse quite nicely to a single curve. The limited 30 atm data reported in Reference (1) is also shown in Figure (14) and can be seen to fall somewhat below the present data curve. Although the cause of this discrepancy is not immediately obvious, the fact that Reference (1) reports 30 atm combustion to have become unstable at an inlet temperature of 600K while no such instability manifested itself in the present tests suggests the possibility of poorly stabilized combustion in Reference (1) and a resulting decrease in residence time at the adiabatic flame temperature.

Figure (15) compares the present 30 atm data curve with the 20 atm data reported in Reference (1). Here, one again sees good collapse of the data when plotted as a function of adiabatic flame temperature and excellent agreement between the 20 atm and 30 atm results, indicating no effect of pressure at these operating conditions.

In Figure (16) the results of the 10 atmosphere tests are plotted as a function of adiabatic flame temperature. In addition to tests at inlet temperatures of 600K and 800K, data is also presented in Figure (16) for an inlet temperature of 727K. These latter data were acquired when the test rig temperature controller malfunctioned, delivering air to the rig at a temperature of 727K rather than the 800K which had been desired. Since the sample probe position during this run was one which would have produced a residence time of two milliseconds had the inlet temperature been 800K, it was necessary to apply a small correction to the data so that it could be compared with the other results on the basis of equal residence time. This was done by computing the actual residence time at the probe station and multiplying the measured emis-

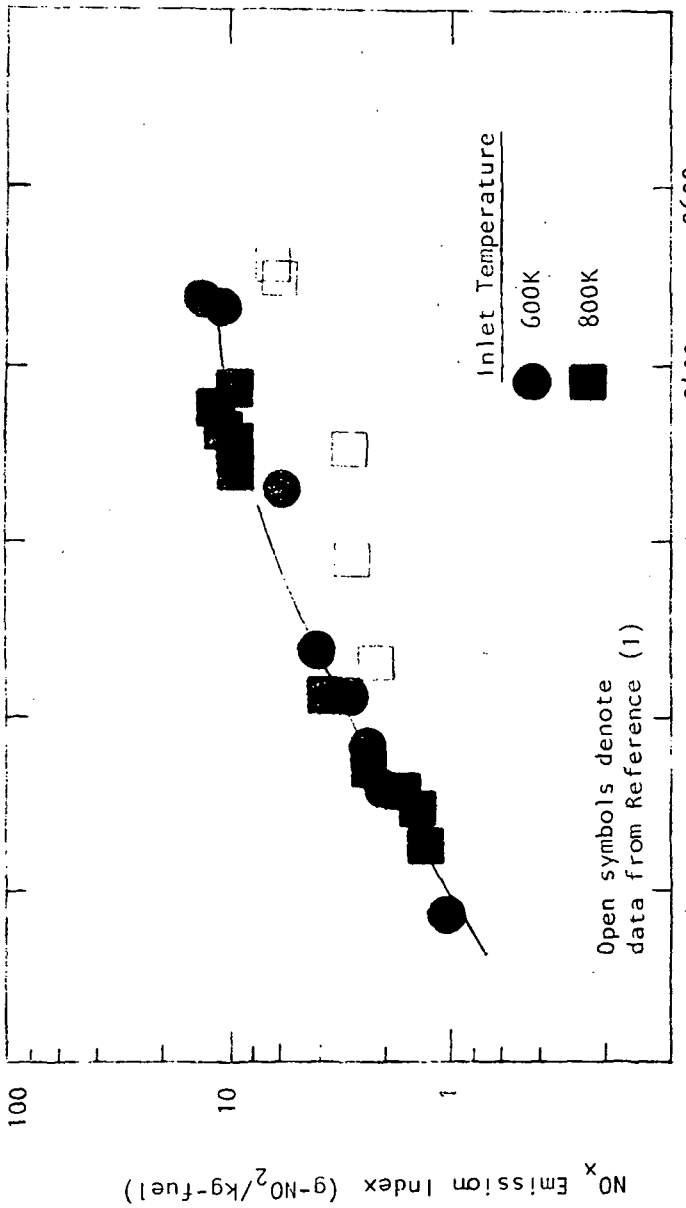

FIGURE 14. CORRELATION OF NO_x EMISSION INDEX FOR 2 MSEC RESIDENCE TIME WITH ADIABATIC FLAME TEMPERATURE (P=30 atm)

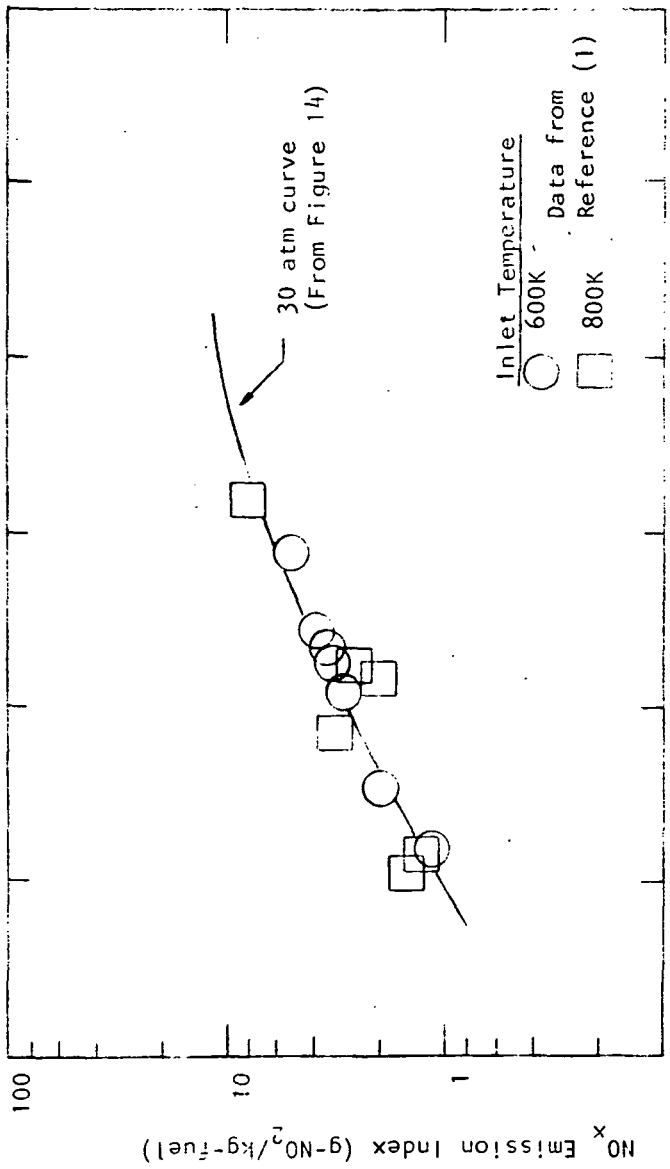

FIGURE 15. COMPARISON OF PRESENT 30 ATM RESULTS WITH 20 ATM DATA OF REFERENCE (1).

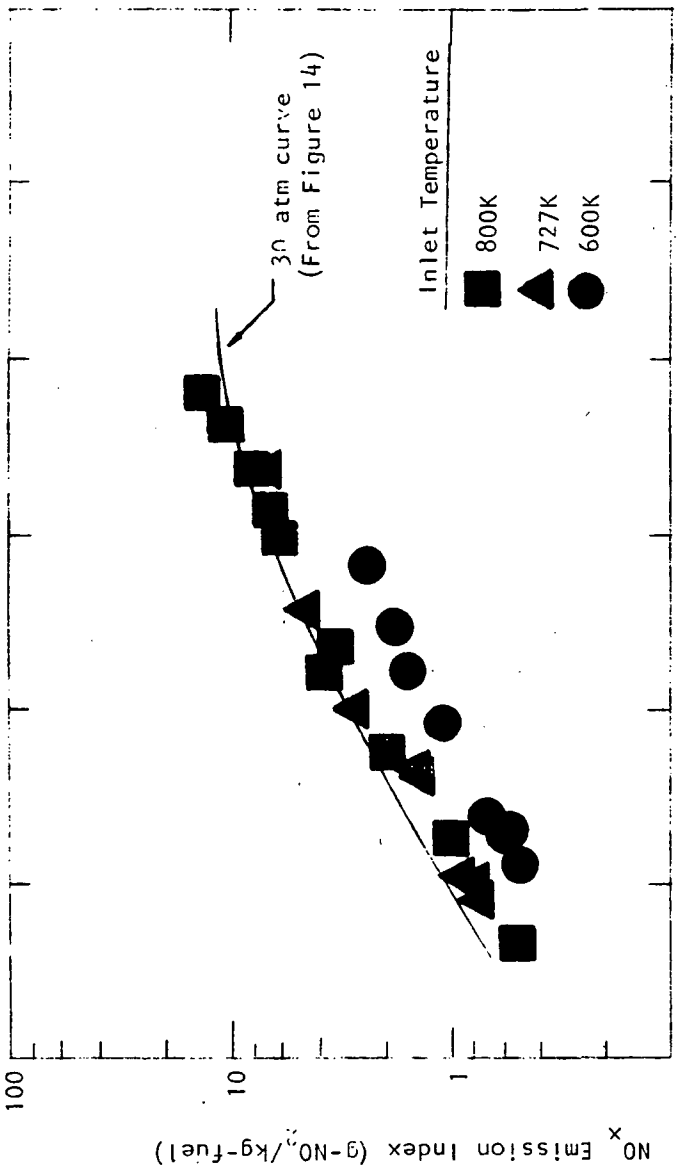

FIGURE 16. CORRELATION OF NO_X EMISSION INDEX FOR 2MSEC RESIDENCE TIME WITH ADIABATIC FLAME TEMPERATURE. (P=10 atm)

sion index by the ratio of two milliseconds to this time. This method of correction assumes a linear rate of NO_x production with time and is based on the measurements of emission index as a function of residence time documented in Reference (1). The maximum correction applied was only 4%, and corresponds to the adiabatic flame temperature error near the lean stability limit.

The 10 atmosphere data of Figure (16) shows a good collapse of the 727K and 800K measurements which fall very close to the 30 atm data curve of Figure (14). The 20 atm/600K data is conspicuous in that it does not collapse to the higher pressure curve, rather running parallel to it but displaced downward. This same data is repeated in Figure (17), this time adding the 10 atmosphere data obtained previously and reported in Reference (1). The data clearly approach the 30 atmosphere curve for inlet temperatures of 727K and higher. The previous data for inlet temperatures of 600K and 800K are lower than those obtained in the current tests. It would appear that the ability to anchor the flame tightly at the flameholder decreases as the pressure and inlet temperature decrease. The present series of experiments, employing a more powerful igniter than was used in Reference (1), apparently produce a more positively stabilized flame. In cases where the flame is not tightly anchored to the flameholder, the assumption of an instantaneious temperature rise in the residence time calculation is clearly invalid. Thus, the downward shift in NO_x level may simply be a reflection of a lower residence time at the adiabatic flame temperature.

Figure (18) compares the present results with data reported in Reference (1) for an inlet pressure of 5 atmospheres. Here again, the higher inlet temperature data collapse to the 30 atmosphere data curve while the 600K inlet temperature data falls below, this time to an even greater degree than occurred at the higher pressure.

From an examination of the data summarized in Figures (14) through (18), it would appear that NO_x emission index is principally a function of adiabatic flame temperature and is not strongly influenced by either equivalence ratio or inlet temperature except insofar as the combination of these two variables

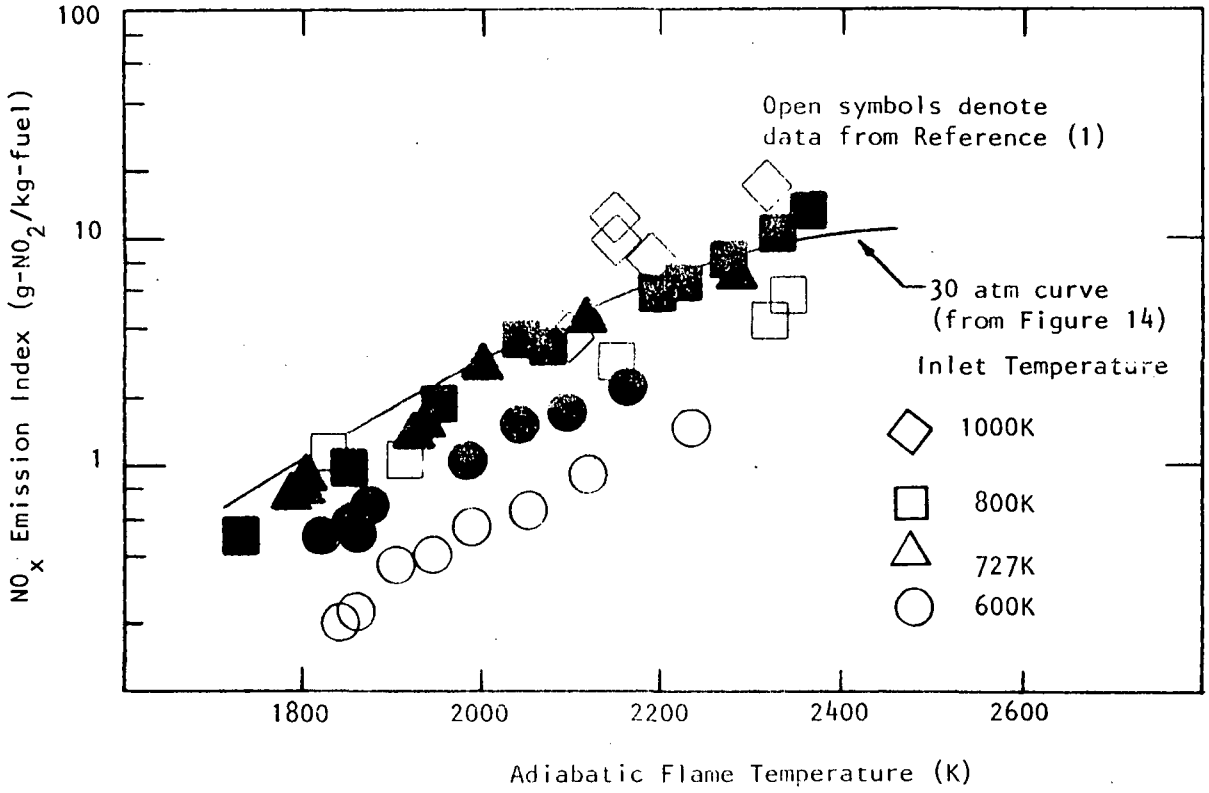

FIGURE 17. CORRELATION OF NO_X EMISSION INDEX FOR 2MSEC RESIDENCE TIME WITH ADIABATIC FLAME TEMPERATURE (P=10 atm)

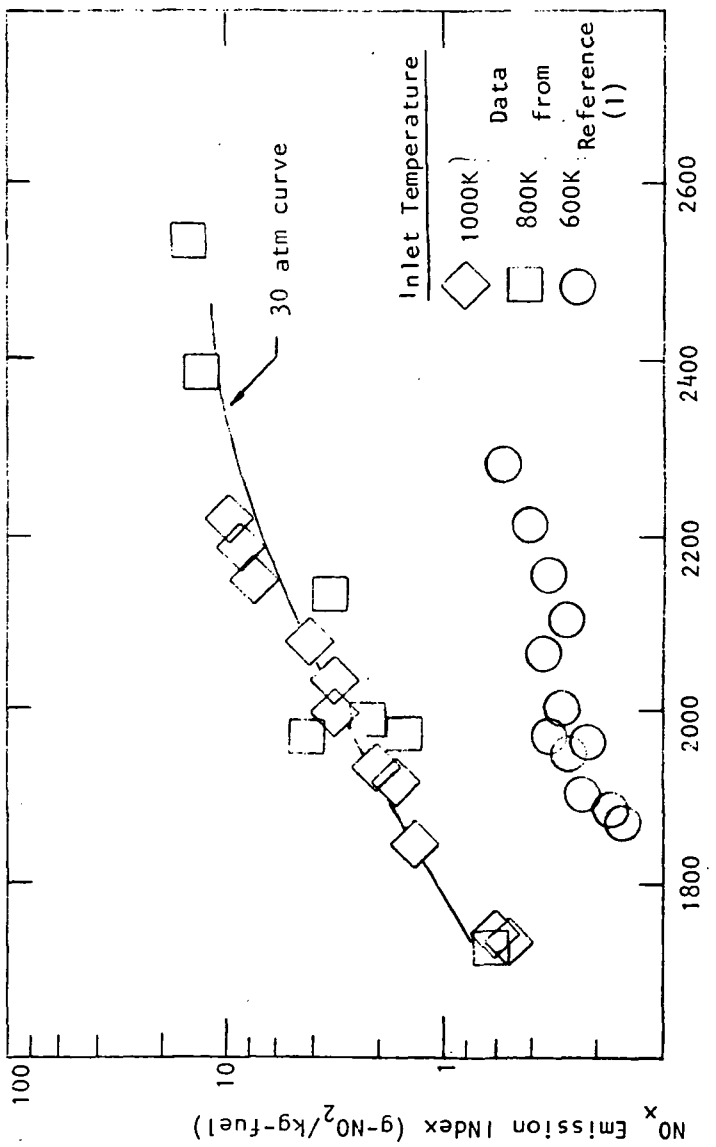

FIGURE 18. COMPARISON OF PRESENT RESULTS WITH 5 ATM NO_X DATA OF REFERENCE (1)

determines the adiabatic flame temperature. Since data reported in Reference (1) indicated that NO_x levels were directly proportional to combustor residence time, the results of this program can be summarized by the following expression:

$$\ln \left(\frac{E_{NO_x}}{\tau}\right) = -72.28 + 2.80\sqrt{T} - \frac{T}{38.02}$$

where E_{NO_x} is the NO_x emission index ($g \cdot NO_2$/kg-fuel), T is the adiabatic flame temperature (K) and τ is the combustor residence time (msec). Over the range of pressures from 5 to 30 atmospheres, there is no significant observed departure from this expression for inlet temperatures of 727K and higher.

SUMMARY OF RESULTS

1. NO_x emission index is principally a function of adiabatic flame temperature and combustor residence time. This function is well represented by the expression

$$\ln \left(\frac{E_{NO_x}}{\tau}\right) = -72.28 + 2.80\sqrt{T} - \frac{T}{38.02}$$

where T is the adiabatic flame temperature (K) and τ is the combustor residence time (msec).

2. Over the range of pressures from 5 to 30 atm, there is no significant effect of pressure on NO_x emission index as a function of adiabatic flame temperature for inlet temperatures above 727K.

3. The three sampling probe designs tested in this study had a pronounced effect on measured CO levels but did not influence NO_x measurements. The most effective probe design for the high pressure conditions prevailing in this study was one which combined thermal and pressure-quenching of the gas sample.

DATA SUMMARY

A. EMISSIONS DATA

P_3 (atm)	T_3 (K)	ϕ CHEM	NO_x (PPM)	UHC (PPMC)	CO (PPM)	E_{NO_x} (g/kg-Fuel)	E_{HC} (g/kg-Fuel)	E_{CO} (g/kg-Fuel)	Adiabatic Flame Temp. (K)
10	600	0.640	35.89	70.52	70	1.47	0.9	1.7	2040
		0.612	23.14	105.8	90	0.99	1.4	2.3	1980
		0.709	57.32	176.3	220	2.12	2.0	5.0	2160
		0.669	43.29	176.3	220	1.69	2.1	5.2	2090
		0.555	13.29	105.8	80	0.62	1.5	2.3	1870
		0.546	12.16	105.8	80	0.58	1.5	2.3	1850
		0.530	9.70	123.4	100	0.47	1.8	3.0	1820
		0.552	10.39	299.7	90	0.49	4.3	2.6	1865
30	600	0.92	368.7	0	730	10.5	0	12.7	2460
		0.63	69.16	0	70	2.87	0	1.76	2020
		0.60	54.7	0	55	2.34	0	1.43	1960
		0.575	44.64	0	65	2.0	0	1.77	1910
		0.508	20.62	20.62	240	1.04	0.39	7.37	1770
		0.927	467.8	0	775	13.4	0	13.5	2470
		0.767	166.3		175	5.7		3.7	2255
		0.661	99.87	74.28	195	3.95	0	4.7	2070
10	800	0.764	346.0	27.5	830	11.92	0.3	17.4	2360
		0.742	291.1	30.65	675	10.31	0.3	14.6	2330
		0.699	202.8	36.06	640	7.6	0.4	14.6	2270
		0.671	159.9	36.06	540	6.23	0.4	12.8	2220
		0.650	142.9	104.6	735	5.74	1.3	18.0	2190

DATA SUMMARY (Continued)

A. EMISSIONS DATA

P_3 (atm)	T_3 (K)	ϕ CHEM	NO_x (PPM)	UHC (PPMC)	CO (PPM)	E_{NO_x} (g/kg-Fuel)	E_{HC} (g/kg-Fuel)	E_{CO} (g/kg-Fuel)	Adiabatic Flame Temp. (K)
10	800	0.583	73.37	180.3	765	3.27	2.4	20.8	2070
		0.566	77.8	185.7	780	3.57	2.6	21.8	2040
		0.521	35.79	119.0	490	1.78	1.8	14.8	1950
		0.467	17.42	140.6	480	0.96	2.4	16.2	1850
		0.446	13.41	165.9	595	0.77	2.9	20.9	1805
		0.411	7.46	284.9	875	0.47	5.4	33.3	1730
30	800	0.74	292	21.16	720	10.2	0.23	15.4	2330
		0.75	313	28.2	310	10.9	0.3	6.55	2345
		0.74	312	10.58	350	10.94	0.11	7.48	2330
		0.75	296	0	420	10.3	0	8.86	2345
		0.73	274	0	370	9.8	0	8.06	2315
		0.767	290	8.82	455	9.84	0.09	9.40	2370
		0.705	262	0	325	9.63	0	7.28	2275
		0.715	260	14.1	400	9.43	0.16	8.84	2290
		0.555	78.8	14.1	200	3.64	0.20	5.64	2020
		0.51	44.69	17.63	285	2.24	0.27	8.70	1940
		0.496	31.46	35.26	475	1.62	0.55	14.93	1910
		0.485	29.18	42.31	470	1.54	0.68	15.1	1890
		0.468	25.08	75.81	415	1.37	1.26	13.81	1850

DATA SUMMARY (Continued)

A. EMISSIONS DATA

P_3 (atm)	T_3 (K)	ϕ CHEM	NO_x (PPM)	UHC (PPMC)	CO (PPM)	E_{NO_x} (g/kg-Fuel)	E_{HC} (g/kg-Fuel)	E_{CO} (g/kg-Fuel)	Adiabatic Flame Temp. (K)
10	727	0.729	173.3	0	1530	6.24	0.0	33.6	2280
		0.689	173.3	17.93	1750	6.59	0.2	40.5	2200
		0.635	101.2	25.10	3720	4.16	0.3	93.1	2110
		0.669	82.86	17.93	4260	3.24	0.2	101.4	2180
		0.570	54.40	10.76	3830	2.48	0.1	106.3	2000
		0.540	28.77	10.76	2440	1.38	0.2	71.4	1935
		0.532	26.25	10.76	2040	1.28	0.2	60.6	1930
		0.469	13.24	17.93	2115	0.73	0.3	70.9	1800
		0.463	11.89	26.90	1640	0.66	0.5	55.7	1785

DATA SUMMARY

B. COMPARISON OF THERMAL, PRESSURE AND PRESSURE/THERMAL QUENCH PROBES

Probe	Reference Velocity, Blockage	ϕ CHEM	NO_x (PPM)	UHC (PPMC)	CO (PPM)	E_{NO_x} (g/kg-Fuel)	E_{HC} (g/kg-Fuel)	E_{CO} (g/kg-Fuel)
Pressure Quench Probe with Moderate Thermal Quench (Figure 7)	35m/s 70%	0.588	120.1	0	15	5.32	0	0.4
		0.569	97.97	0	10	4.47	0	0.3
		0.619	166.7	0	15	7.02	0	0.4
		0.638	193.1	0	15	7.90	0	0.4
		0.644	234.4	0	25	9.51	0	0.6
		0.634	191.6	0	25	7.89	0	0.6
		0.702	297.6	0	40	11.11	0	0.9
		0.717	342.4	0	40	12.52	0	0.9
		0.637	220.1	0	25	9.02	0	0.6
		0.615	190.8	0	20	8.09	0	0.5
		0.563	133.8	0	15	6.17	0	0.4
		0.551	108.3	0	15	5.10	0	0.4
		0.479	56.45	0	5	3.05	0	0.2
		0.432	34.65	0	10	2.07	0	0.4
		0.427	31.79	0	15	1.92	0	0.6
		0.368	17.12	19.02	115	1.19	0.4	4.9
		0.360	14.41	32.33	160	1.03	0.7	6.9
		0.361	13.56	38.04	180	0.97	0.8	7.8

DATA SUMMARY (Continued)

B. COMPARISON OF THERMAL, PRESSURE AND PRESSURE/THERMAL QUENCH PROBES

Probe	Reference Velocity, Blockage	ϕ CHEM	NO_x (PPM)	UHC (PPMC)	CO (PPM)	E_{NO_x} (g/kg-Fuel)	E_{HC} (g/kg-Fuel)	E_{CO} (g/kg-Fuel)
Thermal Quench Probe (Figure 6)	35m/s 70%	0.652	259.2	0	55	10.39	0	1.3
		0.641	226.3	0	45	9.21	0	1.1
		0.758	407.3	0	85	14.13	0	1.8
		0.742	411.4	0	85	14.57	0	1.8
		0.722	376.4	0	75	13.68	0	1.7
		0.650	259.2	0	50	10.41	0	1.2
		0.569	125.7	0	38	5.74	0	1.1
		0.543	95.73	0	34	4.58	0	1.0
		0.457	46.28	0	23	2.61	0	0.8
		0.377	18.13	0	125	1.24	0	5.2
		0.354	11.8	124.4	270	0.86	2.7	11.9
		0.346	11.51	167.1	330	0.85	3.8	14.9

DATA SUMMARY (Continued)

B. COMPARISON OF THERMAL, PRESSURE AND PRESSURE/THERMAL QUENCH PROBES

Probe	Reference Velocity, Blockage	ϕ CHEM	NO_x (PPM)	UHC (PPMC)	CO (PPM)	E_{NO_x} (g/kg-Fuel)	E_{HC} (g/kg-Fuel)	E_{CO} (g/kg-Fuel)
Pressure/ Thermal Quench Probe (Figure 8)	35m/s 70%	0.716	400.	10.34	400	14.65	0.1	8.9
		0.702	371.7	12.07	360	13.87	0.1	8.2
		0.684	297.3	12.07	300	11.38	0.1	7.0
		0.656	257.3	12.07	220	10.24	0.1	5.3
		0.609	196.6	12.07	140	8.42	0.2	3.6
		0.558	106.5	13.78	65	4.96	0.2	1.8
		0.477	52.61	13.78	35	2.85	0.2	1.2
		0.473	49.75	13.78	30	2.72	0.2	1.0
		0.394	22.87	13.78	135	1.49	0.3	5.4
		0.389	20.0	13.78	150	1.21	0.3	6.0